PeAPA | Publicación Electrónica
ASOCIACIÓN PALEONTOLÓGICA ARGENTINA

www.peapaleontologica.org.ar

Paleontological record of a Gondwana Cretaceous paleolake as proxy for paleoclimate reconstruction

CECILIA ANDREA BENAVENTE[1,2]
JUAN I. BALAGUER GASULL[3]
PAULA GUILLERMINA GIORDANO[3]
ADRIANA CECILIA MANCUSO[1]
ANDREA BEATRIZ ARCUCCI[3]

1. Instituto Argentino de Nivología, Glaciología y Ciencias Ambientales (IANIGLA), CCT-Mendoza, Consejo Nacional de Investigaciones Científicas y Técnicas (CONICET). Av. Adrián Ruiz Leal s/n, Parque General San Martín CC 330, 5500 Mendoza, Mendoza, Argentina.
2. Geología, Facultad de Ciencias Exactas y Naturales (FCEN), Universidad Nacional de Cuyo (UNCuyo). Padre Jorge Contreras 1300, 5502 Mendoza, Mendoza, Argentina.
3. Área de Zoología, Facultad de Química Bioquímica y Farmacia (FQByF), Universidad Nacional de San Luis (UNSL). Ejército de Los Andes 950, 5700 San Luis, San Luis, Argentina.

Recibido: 25 de enero 2023 - **Aceptado:** 17 de abril 2023 - **Publicado:** 09 de agosto 2023

Para citar este artículo: Cecilia Andrea Benavente, Juan I. Balaguer Gasull, Paula Guillermina Giordano, Adriana Cecilia Mancuso, & Andrea Beatriz Arcucci (2023). Paleontological record of a Gondwana Cretaceous paleolake as proxy for paleoclimate reconstruction. *Publicación Electrónica de la Asociación Paleontológica Argentina* 23 (2): 81–96.

Link a este artículo: http://dx.doi.org/10.5710/PEAPA.17.04.2023.454

ISSN 2469-0228

Asociación Paleontológica Argentina
Maipú 645 1° piso, C1006ACG, Buenos Aires
República Argentina
Tel/Fax (54-11) 4326-7563
Web: www.apaleontologica.org.ar

Publicación Electrónica
ASOCIACIÓN PALEONTOLÓGICA ARGENTINA
Año 2023 - 23(2): 81–96
ARTÍCULO

PALEONTOLOGICAL RECORD OF A GONDWANA CRETACEOUS PALEOLAKE AS PROXY FOR PALEOCLIMATE RECONSTRUCTION

CECILIA ANDREA BENAVENTE[1,2], JUAN I. BALAGUER GASULL[3], PAULA GUILLERMINA GIORDANO[3], ADRIANA CECILIA MANCUSO[1], AND ANDREA BEATRIZ ARCUCCI[3]

[1]Instituto Argentino de Nivología, Glaciología y Ciencias Ambientales (IANIGLA), CCT-Mendoza, Consejo Nacional de Investigaciones Científicas y Técnicas (CONICET). Av. Adrián Ruiz Leal s/n, Parque General San Martín CC 330, 5500 Mendoza, Mendoza, Argentina. *cebenavente@gmail.com*; *amancu@mendoza-conicet.gob.ar*

[2]Geología, Facultad de Ciencias Exactas y Naturales (FCEN), Universidad Nacional de Cuyo (UNCuyo). Padre Jorge Contreras 1300, 5502 Mendoza, Mendoza, Argentina. *ceciliabenavente@fcen.uncu.edu.ar*

[3]Área de Zoología, Facultad de Química Bioquímica y Farmacia (FQByF), Universidad Nacional de San Luis (UNSL). Ejército de Los Andes 950, 5700 San Luis, San Luis, Argentina. *balaguerjuani@gmail.com*; *guillerminagiordano@gmail.com*; *andrea.arcucci@gmail.com*

CAB: https://orcid.org/0000-0002-3414-0330; **PGG:** https://orcid.org/0000-0001-8816-4808; **ACM:** https://orcid.org/0000-0002-0264-3806; **ABA:** https://orcid.org/0000-0001-8098-1512

Abstract. The La Cantera Formation (Aptian) represents an underfilled lake system developed in an extensional basin during the Cretaceous hothouse and it bears an abundant and diverse fossil record. Our goal was to investigate paleoclimate conditions of the unit from a multiproxy approach. We analyzed two proxies: a) the stable isotope (carbon and oxygen) composition of basal Actinopterygii and Neopterygii fish remains and from indeterminate plant remains; and b) the clay mineral assemblage composition; providing two independent lines of evidence to reconstruct paleoclimate conditions including paleotemperature calculations for lake waters. The values obtained for fish remains for $\delta^{13}C$ range between -8.4 and -1.3 ‰ ($\delta^{13}C = \chi$ -5.57‰; $\sigma \pm 2.25$); and $\delta^{18}O$ values that vary between -5.7 and -3.6‰ ($\delta^{18}O = \chi$ -4.33‰; $\sigma \pm 0.84$); in the case of plant remains $\delta^{13}C$ values range between -25.8 and -22.8‰ ($\delta^{13}C = \chi$ -25‰ -4.33). Paleotemperatures obtained from $\delta^{18}O$ for the water column ranged between 23.33 to 35.80 °C. Plant $\delta^{13}C$ signature allowed obtaining a $\delta^{13}C_{CO2}$ composition of -5 ‰. This agrees with the interpretation of the La Cantera originating from sediment deposition in an underfilled lake basin and with the global climate context of the Cretaceous. The clay mineral assemblage is dominated by illite-smectite indicating enhanced hydrolysis and seasonal rainfall supporting temporal warmup of the lake. Our data supports aridity conditions during the La Cantera paleolake existence. These findings suggest that geochemical proxies of paleontological datasets are accurate for paleoclimate reconstructions for the deep time records of the La Cantera lacustrine system.

Key words. La Cantera Formation. Lacustrine. Underfilled lake. Stable isotopes. Fossil fish. Fossil plant.

Resumen. REGISTRO PALEONTOLÓGICO DE UN PALEOLAGO CRETÁCICO DE GONDWANA COMO PROXY PARA RECONSTRUCCIONES PALEOCLIMÁTICAS. La Formación La Cantera representa un sistema lacustre *underfilled* desarrollado en una cuenca extensional durante la casa cálida del Cretácico y posee un registro fósil abundante y diverso. Investigamos las condiciones paleoclimáticas para la unidad desde un enfoque multiproxy. Analizamos dos proxies: a) la composición isotópica del carbono y del oxígeno de peces Actinopterygii basales y Neopterygii y de restos de plantas; y b) la composición de los ensambles de arcillas; aportando líneas de evidencia independientes a la reconstrucción paleoclimática. Los valores obtenidos para peces de $\delta^{13}C$ varían entre -8.4 y -1.3‰ ($\delta^{13}C = \chi$ -5.57‰; $\sigma \pm 2.25$); y para $\delta^{18}O$ varían entre -5.7 y -3.6‰ ($\delta^{18}O = \chi$ -4.33‰; $\sigma \pm 0.84$); en el caso de las plantas varían entre -25.8 y -22.8‰ ($\delta^{13}C = \chi$ -25‰; $\sigma \pm 4.33$). Las paleotemperaturas obtenidas a partir del $\delta^{18}O$ para la columna de agua fueron de 23.33 a 35.80 °C. La firma isotópica del $\delta^{13}C$ de las plantas permitió obtener la composición de $\delta^{13}C_{CO2}$ de -5 ‰. Esto concuerda con la interpretación de que La Formación Cantera pudo haberse originado a partir de la depositación de sedimentos en un paleolago *underfilled* y con el contexto paleoclimático global del Cretácico. Los ensambles de arcillas están dominados por illita-esmectita indicando un índice de hidrólisis elevado y estacionalidad en las precipitaciones lo que apoya el calentamiento temporal del cuerpo de agua. Estos datos indican condiciones de aridez durante la existencia del paleolago La Cantera y sugieren que los proxies geoquímicos de las bases de datos paleontológicas son precisos para la reconstrucción del paleoclima local en tiempo profundo de la Formación La Cantera.

Palabras clave. Formación La Cantera. Lacustre. Lago *Underfilled*. Isótopos estables. Peces fósiles. Plantas fósiles.

SEDIMENTARY records (biotic and abiotic) are useful tools with high fidelity for paleoenvironmental and paleoclimate reconstructions, being lacustrine deposits the highest fidelity archives in the sedimentary record for terrestrial paleoecosystems, since they condense local and regional data that can be used as proxies of the environmental and

climate conditions of the past (Gierlowski-Kordesch & Kelts, 1994). Such datasets have been applied successfully for Quaternary system reconstructions and deep time systems as well (*e.g.*, Abell *et al.*, 1982; Wang *et al.*, 2002; Benavente *et al.*, 2021, 2022). Among the data preserved in lacustrine records, there are clay assemblages of the fine-grained deposits of lake basins that can be applied for such studies as well as the geochemical signature of stable isotopes (*e.g.*, Benavente *et al.*, 2019, 2021; Salduondo *et al.*, 2022). The stable isotope signature in a lacustrine system can provide information about external (precipitation) and internal processes (stratification) (Leng *et al.*, 2005). Stable isotopes can also explore the different resources availability for the organisms that inhabit the system and how they exploit them (Longinelli & Nuti, 1973; Kolodny *et al.*, 1983; Gröcke, 2002; West *et al.*, 2006; Cerling *et al.*, 2007), like the food source or the niche they inhabit in the body of water (shallow marginal versus more profundal) (Pereira *et al.*, 2021).

La Cantera Formation (Sierra del Gigante, San Luis Province) is a unit that represents a lacustrine system. Their sediments were deposited during Aptian times in an extensional tectonic context (Flores, 1969; Criado Roque *et al.*, 1981; Rivarola & Spalletti, 2006). It bears a rich fossil record with high fidelity preservation that includes fish, plant (micro and macro), and insects (Puebla *et al.*, 2012; Arcucci *et al.*, 2015; Castillo Elías, 2016; Giordano *et al.*, 2016). Even more, there is a study of the fossil record of the unit to infer paleoclimate conditions (Prámparo *et al.*, 2018). Nevertheless, single proxy analysis has limitations and linked to the fossil record such proxy presents strong biases like preservation of the remains and other factors controlling their distribution, like local climate conditions instead of regional ones (Benavente *et al.*, 2022). Therefore, coupling different proxies such as the geochemical composition of fossils and clay assemblage composition can be more accurate for environmental inferences. The isotopic signature of fossils is highly conservative in the sedimentary record and allows identifying environmental patterns that affected organisms in the system they inhabited (West *et al.*, 2006; Tütken *et al.*, 2006; Rey *et al.*, 2020; Pereira *et al.*, 2021). For instance, the chemical composition of ganoid scales is generally used for robust paleohydrology and paleoclimate reconstructions (Iacumin *et al.*, 1996; Grimes *et al.*, 2003; Tütken *et al.*, 2006; Amiot *et al.*, 2010; Pucéat *et al.*, 2010; Sisma-Ventura *et al.*, 2019).

The La Cantera lacustrine system has been interpreted as an underfilled lake basin type (Castillo-Elías, 2016) according to Bohacs *et al.* (2000). This implies that it was characterized by an evaporative facies association, which is coherent with, among other diagnostic features, significant gypsum deposits found throughout the unit associated with mud cracks (Castillo-Elías, 2016). However, development of underfilled lake basins is not only controlled by paleoclimate alone but by hydrological factors (Benavente *et al.*, 2019). This provides an interesting setting to reconstruct paleohydrological conditions of such an evaporative system.

The main goals of this study are: a) to test new geochemical proxies that can be extracted from the fossil record such as the stable isotope composition (carbon and oxygen) of fish and plant remains; and b) to obtain the clay assemblage composition in order to provide a multiproxy interpretation for paleoenvironmental and paleoclimate conditions of the La Cantera lacustrine system during the Aptian.

Geological Setting

The San Luis Basin is located in the Southwest margin of the Sierras Pampeanas geological province, limiting to the Northwest with the Sierra Grande de San Luis Province (Yrigoyen, 1975). To the west, it extends up to the Bolsón del Desaguadero (Mendoza Province) and to the north it is identified up to the Southwest limit of the San Juan Province (Fig. 1.1). The infilling of the basin is entirely continental and comprehends Aptian to Neogene deposits including the La Cantera Formation, that reaches up to 40 m in thickness at the basin center (Fig. 1.2). This unit outcrops at the Sierra del Gigante (Northwest of the San Luis Province) (Fig. 1.3) and represents a lacustrine system. These deposits are characterized by dominant ripple-cross sandstone and dark finely-laminated mudstone (Fig. 1.4) with abundant fossil remains (Flores, 1969; Prámparo, 1994; Castillo Elías, 2016).

The fossil record of the La Cantera Formation includes crustaceans (ostracods and conchostracans), insects, actinopterygian fish, algae, and micro- and macroflora (briophyta, monilophytes, equisetaleans, gnetaleans, and

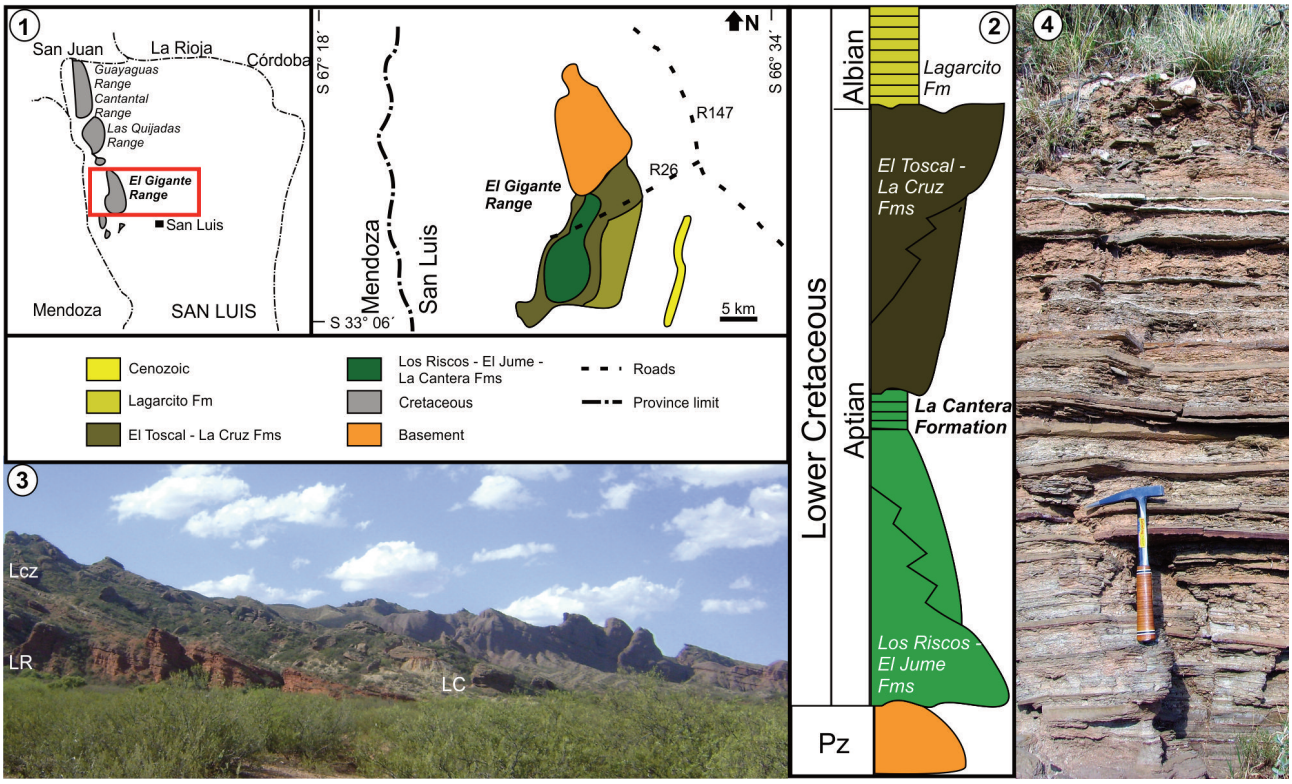

Figure 1. 1, Geological map of the San Luis Basin. Modified from Arcucci *et al.* (2015). **2,** Stratigraphy of the El Gigante Group (Aptian–Albian), modified from Arcucci *et al.* (2015). **Pz,** Paleozoic. **3,** Outcrop photograph showing the Los Riscos **(LR)**, La Cantera **(LC)**, and La Cruz **(Lcz)** formations at the Sierra del Gigante deposits. **4,** Field photograph of the La Cantera Formation at its type locality, where it is mostly constituted of dark, well-laminated mudstones interbedded with fine-grained sandstone.

angiosperms) (Petrulevicius *et al.*, 2010; Arcucci *et al.*, 2015; Giordano *et al.*, 2016). The palynology assemblage has allowed to link the deposits to the Late Aptian (Prámparo, 2012). The micro- and macroflora assemblage of *Ephedripites* sp., *Cycadopites* sp., *Monosulcites* sp., and *Classopollis* sp. has allowed also a single proxy paleoclimate inference of aridity indicators (Puebla *et al.*, 2012), with briophyta indicating local humidity (Puebla, 2009).

MATERIALS AND METHODS

A high-resolution stratigraphic log of the middle section of the La Cantera Formation was measured at 1:100 scale at the type locality "La Cantera de Gutierrez" (Sierra del Gigante) (32° 59′ 23.8" S; 66° 52′ 52.6" W). Six levels were sampled and hand samples were collected for fossil extraction and eight mudstone levels were sampled for clay assemblage analysis.

Materials

Fish. Two groups of fish remains were analyzed with low magnification binocular microscope (Leica M80) at the fossil repository at the Universidad Nacional de San Luis (UNSL): 1) basal Actinopterygii up to 10 cm long and 2) ganoid Neopterygii up to 5.5 cm average of total length. The specimens were well preserved and they are housed at the Museo Interactivo de Ciencias (MIC), UNSL collection (Figs. 2.1–3).

For this study, uncatalogued specimens were used, since most of them were destroyed during sampling. Samples were taken from teeth and bones (Tab. 1) of nine basal Actinopterygii specimens (field number: C1, C2, C3, C4, C5A, C5B, C7, C8, and SLC2018) and from bones, fin elements, scutes, and scales of nine ganoid Neopterygii specimens (MIC-V707; and field number: T1, T4, T5, T6, T7, T8, T9, and TB2).

Macroflora. Five samples of indeterminate stem remains have been analyzed (Fig. 2.4).

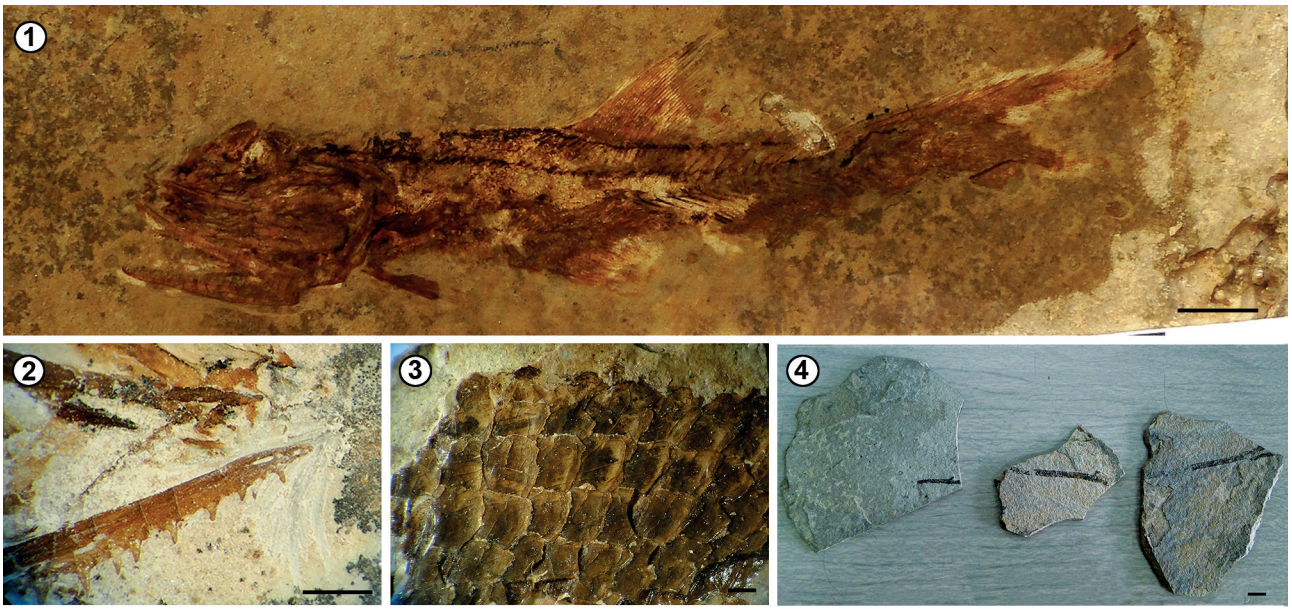

Figure 2. Images of fossils selected for sampling. **1,** Articulated basal Actinopterygii. Scale bar= 5 mm. **2,** Maxilar bone and teeth from a basal Actinopterygii. Scale bar= 1 mm. **3,** Patch of scales from a ganoid Neopterygii. Scale bar= 1 mm. **4,** Plant remains. Scale bar= 1 cm.

Methods

Carbon and oxygen stable isotopes. Carbon and oxygen stable isotopes were sampled from fish and plant remains. These samples were analyzed on a Thermo Fisher Scientific GasBench II, equipped with a PAL autosampler, and coupled to a ConFlow IV interface and a MAT 253 mass spectrometer (Thermo Fisher Scientific), to determine their carbon and oxygen isotopic compositions ($\delta^{13}C$ and $\delta^{18}O$) at the Stable Isotope Ratio Facility for Environmental Research, University of Utah, Salt Lake City, Utah, USA.

The samples were weighed using a Sartorious microbalance and loaded into 4.5 mL flat-bottomed borosilicate vials (Labco) and capped with Labco butyl rubber septa. Then, the vials were flushed for six min on a PAL autosampler with ultrahigh-purity grade helium (99.999% He) at a flow rate of 50 mL/min. During flushing, the vials were kept in a heated (50 °C) aluminum block. The samples were reacted with 10 droplets of phosphoric acid (H_3PO_4) (kept at 50 °C) to produce CO_2 gas. The samples were allowed to equilibrate for 12 h before analysis. During analysis, the CO_2 gas produced in the vials was collected using a sampling loop of 100 µL and then transported to the mass spectrometer. Nine individual injections per analysis were made for each sample, and for reference materials, and their average was taken as the final number. Three sets of internal reference materials were used to calibrate the system and our samples. Carrara marble, LSVEC, and Marble-Std were used as primary reference materials, and Marble-Std was used as a secondary reference material to cross-check the final number. Internal reference materials were calibrated against international standards NBS-18 and NBS-19. Values are reported as per mil relative to the Vienna Peedee belemnite (VPDB) standard. Precision was better than 0.05‰ for $\delta^{18}O$ and 0.02‰ for $\delta^{13}C$.

Mineralogical analysis. Mineralogical composition of bulk and the oriented 2 µm size fraction of the eight mudstone samples (M1/18-M8/18) was analyzed through X-ray diffraction (XRD) analysis at the Centro de Investigaciones Geológicas in La Plata City, Buenos Aires Province, Argentina, using a Panalytical X'PERT Pro diffractometer equipment following Moore & Reynolds (1997). The eight rock samples were disaggregated and powdered in an agate mortar. Clay minerals (Tab. 2) were obtained by pipetting the fraction <2 µm in a suspension with distilled water following the Stokes Law. The samples were prepared according to the glass slide method: a) natural, air-dried sample in the laboratory at environment temperature; b) glycolated, sample exposed to the vapors of an ethylene glycol solution for at

TABLE 1 – $\delta^{13}C$ and $\delta^{18}O$ values from fish and plant remains, paleotemperature calculations and $\delta^{13}C_{CO2}$ composition of the La Cantera Formation, Aptian, Sierra del Gigante, San Luis Province, Argentina

Sample	Level	Fossil group	Tissue	$\delta^{13}C_{VPDB}$ (‰)	σ	$\delta^{18}O_{VPDB}$ (‰)	σ	$\delta^{18}O_{PO4\ VSMOW}$ (‰)	T(°C)	$\delta^{13}C_{CO2}$
C8	-	Basal Actinopterygii	Jaw and teeth	-7.2	0	-4.1	0.1	10.15	46.61	-
T9	-	Ganoid Neopterygii	Scales	-7.1	0.1	-4.1	0.2	13.24	33.09	-
T1	0	-	Scute and fulcrum	-7.3	0.2	-5.7	0.3	13.41	32.3	-
T4	1	Ganoid Neopterygii	Scales	-1.3	0.1	-4.7	0.1	-	-	-
T5		-	-	-8.4	0	-4.7	0.2	11.64	40.06	-
C1	2	Basal Actinopterygii	Bones	-3.6	0	-4.6	0	12.61	35.8	-
C4		-	Jaw and teeth	-7.1	0.1	-5.1	0.1	15.46	23.33	-
C5A		-	-	-7.6	0.2	-5.3	0.1	14.49	27.57	-
C7		-	-	-6.2	0.1	-5.3	0.1	11.13	42.29	-
C5B		-	-	-1.7	0	-3.5	0.1	13.0	34.17	-
T7		Ganoid Neopterygii	Bones	-2.1	0	-3.8	0	10.32	45.85	-
T8			Scales	-5.9	0	-4.6	0	14.31	28.36	-
T6			-	-4.1	0.1	-4.4	0.1	13.53	31.79	-
T2B	3	Ganoid Neopterygii	Rays	-6	0.1	-2.2	0.1	-	-	-
C2	4	Basal Actinopterygii	Jaw and teeth	-5.7	0	-3.7	0.1	13.93	-	-
C3				-8.2	0.1	-4.3	0.1	-		
MIC-V707	9	Ganoid Neopterygii	Scales	-5.2	0.2	-3.6	0.1	-	-	-
SLC2018	-	Basal Actinopterygii	Jaw and teeth	-9	0.0	-4.8	0.1	9.5	49.45	-
P0	-	Indet plant fragment	Stem	-26.2	-	-	-	-	-	-5.9
P1	9	Indet plant fragment	Stem	-26.3	-	-	-	-	-	-6.1
P4	-	Indet plant fragment	Stem	-25.8	-	-	-	-	-	-5.6
P7	-	-	-	-25.1	-	-	-	-	-	-4.9
P9	2	Indet plant fragment	Stem	-22.8	-	-	-	-	-	-2.6

TABLE 2 – Bulk rock mineralogy of mudstones from the La Cantera Formation, Aptian, Sierra del Gigante, San Luis Province, Argentina

Sample	Ka	Il	I/S	Sm	Ch	An	Qz	Fs	Pl	Ca	Py
M8/18		xx	x		x	x	x	x	x		
M7/18	x	xx	x	x	x	x	x	x	x	xx	
M6/18	x	xx			x	x	x	x	x	xx	
M5/18	x	xx	x	x	x	x	x	x	x	xx	
M4/18	x	xx			x	x	x	x	x	xx	
M3/18	x	xx	x		x	x	xx	x	x	xx	x
M2/18	x	xx	x		x	x	x	x	x	xx	
M1/18	x	xx	x		x	x	xx	x	x	x	

Abbreviations: An, analcime; **Ca,** calcite; **Ch,** chlorite; **Fs,** feldspar; **Ka,** kaolinite; **Il,** illite; **I/S,** interstratified illite/smectite; **Pl,** plagioclase; **Py,** pyrite;**Qz,** quartz; **Sm,** smectite; **x,** presence; **xx,** high intensity XRD peak.

least 24 h; and c) calcined, the sample taken at 550 °C for two hours. X-ray diffraction patterns were obtained using Cu K-alpha radiation (kα =1.5403 Å) operated at 40 kV, 40 mA, and scanning speed of 0.04°/s, between 4° to 37° 2θ, for the total rock samples; among 2° to 32° for the natural samples of the clay fraction; 2° to 27° for the glycolated samples of that same fraction, and 3° to 15° for the calcined samples. The identification of main mineral phases and clay minerals was based on diagnostic peaks according following Moore & Reynolds (1997).

Diagenesis assessment

In order to determine the diagenetic overprint of the isotopic signature, the correlation coefficient between $\delta^{18}O_{CO3}$ and $\delta^{18}O_{PO4}$ was analyzed for the samples (Iacumin, 1996; Michener & Lajtha, 2008), using the software STATISTICA (StatSoft, TIBCO Software, Windows).

Paleotemperature calculation

It was done following the equation from Longinelli & Nuti (1973) and modified by Tütken *et al.* (2006) for fish teeth:

$$T°_{H2O}(°C) = 113.4 - 4.38\,(\delta^{18}O_{PO4}(V_{SMOW}) - \delta^{18}O_{H2O}(V_{SMOW})$$

Following the criteria from Benavente *et al.* (2021, 2022), the $\delta^{18}O$ of modern meteoric water was obtained from Waterisotopes.org (http://wateriso.utah.edu/waterisotopes/pages/data_access/oipc.html) (Bowen & Wilkinson, 2002), inputting latitude and altitude. Paleolatitude was calculated for the basin during the Cretaceous from the Paleolatitude Calculator for Paleoclimate Studies (http://www.paleolatitude.org/) (van Hinsbergen *et al.*, 2015) but calculation showed no significant difference with modern latitude; therefore, modern coordinates were used (32° 49′ S; 66° 59′ W). Paleoaltitude was inferred as approximately 500 masl according to the development of rift lakes in the modern East Africa Rift (Bessems *et al.*, 2008; Bergner *et al.*, 2009; Moernaut *et al.*, 2010).

We applied the Kolmogorov-Smirnov statistical test to the distribution of the data using Excel (Microsoft, Windows). Data distribution of both variables ($\delta^{18}O$, $\delta^{13}C$) was normal; therefore, the Pearson correlation coefficient was calculated using InfoStat 2020 software (Universidad Nacional de Córdoba, Windows, Córdoba).

$\delta^{13}C_{CO2}$ calculation

It was done following the equation from Farquhar *et al.* (1989) simplified in Gröcke (2002), assuming linear isotopic fractionation:

$$\delta^{13}C_{air}(‰) = \delta^{13}C_{plant} + 20.22$$

We also applied the equation proposed by Arens & Jahren (2000) to test the better fit to the dataset:

$$\delta^{13}C_{CO2} = (\delta^{13}C_{plant} + 18.67)/1.10$$

RESULTS

C and O stable isotopes from fossil remains

Fish samples from the La Cantera Formation have $\delta^{13}C$ values that range between -8.4 and -1.3‰ ($\delta^{13}C_{Act} = \chi$ -5.57; $\sigma \pm 2.25$); and $\delta^{18}O$ values that vary between -5.7 and -3.6‰ ($\delta^{18}O_{Act} = \chi$ -4.33‰; $\sigma \pm 0.84$) (Fig. 3, Tab. 1). Average values of $\delta^{13}C$ and $\delta^{18}O$ for both fish groups are very similar ($\delta^{13}C_{Act} = \chi$ -5.91‰; $\sigma \pm 2.21$; $\delta^{13}C_{Neop} = \chi$ -5.26‰; $\sigma \pm 2.38$; $\delta^{18}O_{Act} = \chi$ -4.48‰; $\sigma \pm 0.7$; $\delta^{18}O_{Neop} = \chi$ -4.2‰; $\sigma \pm 0.96$) (Fig. 3; Tab. 1).

Interpretation. Since both groups present similar averages in their isotopic signature, biological effects (metabolic or physiologic) are discarded. There are no significant differences either when comparing the different materials analyzed (bones, teeth, scales) (Tab. 1). One interpretation is that there is no difference in the fractionation effect for different tissues in the organisms analyzed or alternatively perhaps, this effect has been homogenized by secondary imprint (diageneses and/or weathering) of the signature (Tieszen *et al.*, 1983).

Diagenesis analysis

There is a low negative correlation for fish values between $\delta^{18}O_{CO3}$ y $\delta^{18}O_{PO4}$, with a correlation coefficient of r = -0.28 (Fig. 4.1). The correlation analysis by the taxonomic group of fish shows a similar result, with a correlation coefficient of r = -0.41 for basal Actinopterygii (Fig. 4.2) and r = -0.39 for ganoid Neopterygii (Fig. 4.3) and also for the different tissues sampled (Fig. 4.4).

Interpretation. The correlation coefficients obtained for the

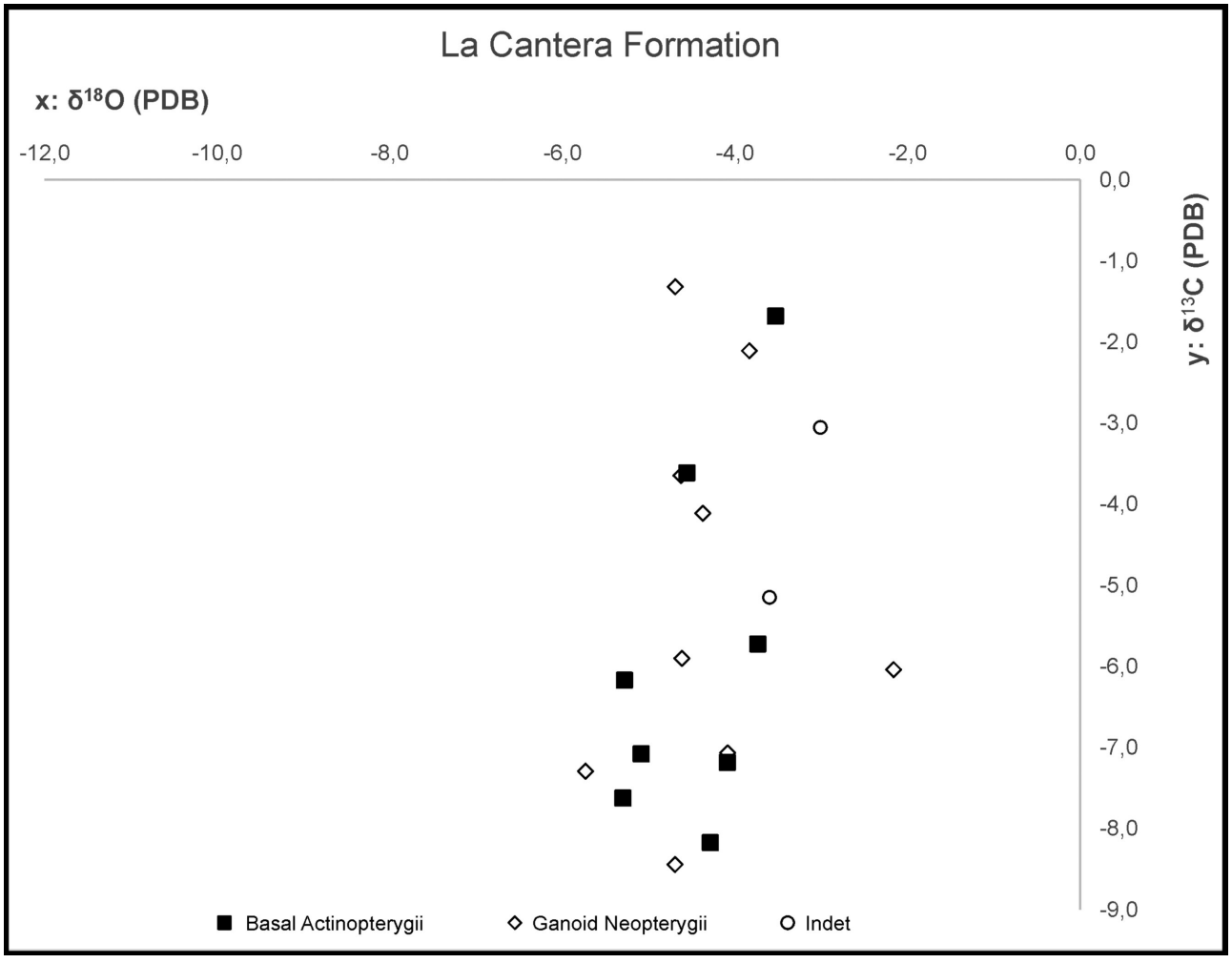

Figure 3. Cross-plot of $\delta^{18}O$ and $\delta^{13}C$ data of the fossil record (fish) of the La Cantera Formation (Aptian), San Luis Basin in the San Luis Province, Argentina.

complete fish remains dataset, each group separately, and even for different tissue types suggest that the stable isotope signature has been diagenetically altered (Kolodny *et al.*, 1983; Iacumin *et al.*, 1996; Tütken *et al.*, 2006). Therefore, the fish remains dataset wouldn´t be completely reliable for paleoclimate reconstructions.

Paleotemperature

Paleotemperatures obtained using $\delta^{18}O_{PO4}$ values from fish remains vary between 23.33 °C and 49.43 °C (Tab. 1).

Interpretation. Within the dataset, we consider that the warm end member presents unreasonable water column values for fish to inhabit (Grande, 2010). Considering the diagenesis analysis that suggests the primary isotopic signature might have been altered, we consider that the most likely primary data set is the one resulting in a paleothermal range of 23.33 °C and 35.8 °C. This implies discarding five values from samples from basal Actinopterygii and ganoid Neopterygii, because they were most likely subject to diagenetic reset. Since this effect is potentially observed in different tissues and different stratigraphic levels, no clear diagenetic pattern can be inferred.

Plant samples have $\delta^{13}C$ values that range between -25.8 and -22.8‰ ($\delta^{13}C_p$ = -25χ; σ ± 4.33) (Tab. 1).

Interpretation. The $\delta^{13}C$ signature of plant remains is very similar to modern C3 plants that show an average of -25.4‰ and vary between -22.5‰ and -27.9‰ (Craig, 1954; Gröcke, 2002). Our data are consistent with $\delta^{13}C$ wood values (Gröcke, 2002). This suggests a high-fidelity preservation of the C stable isotope signature in this data set.

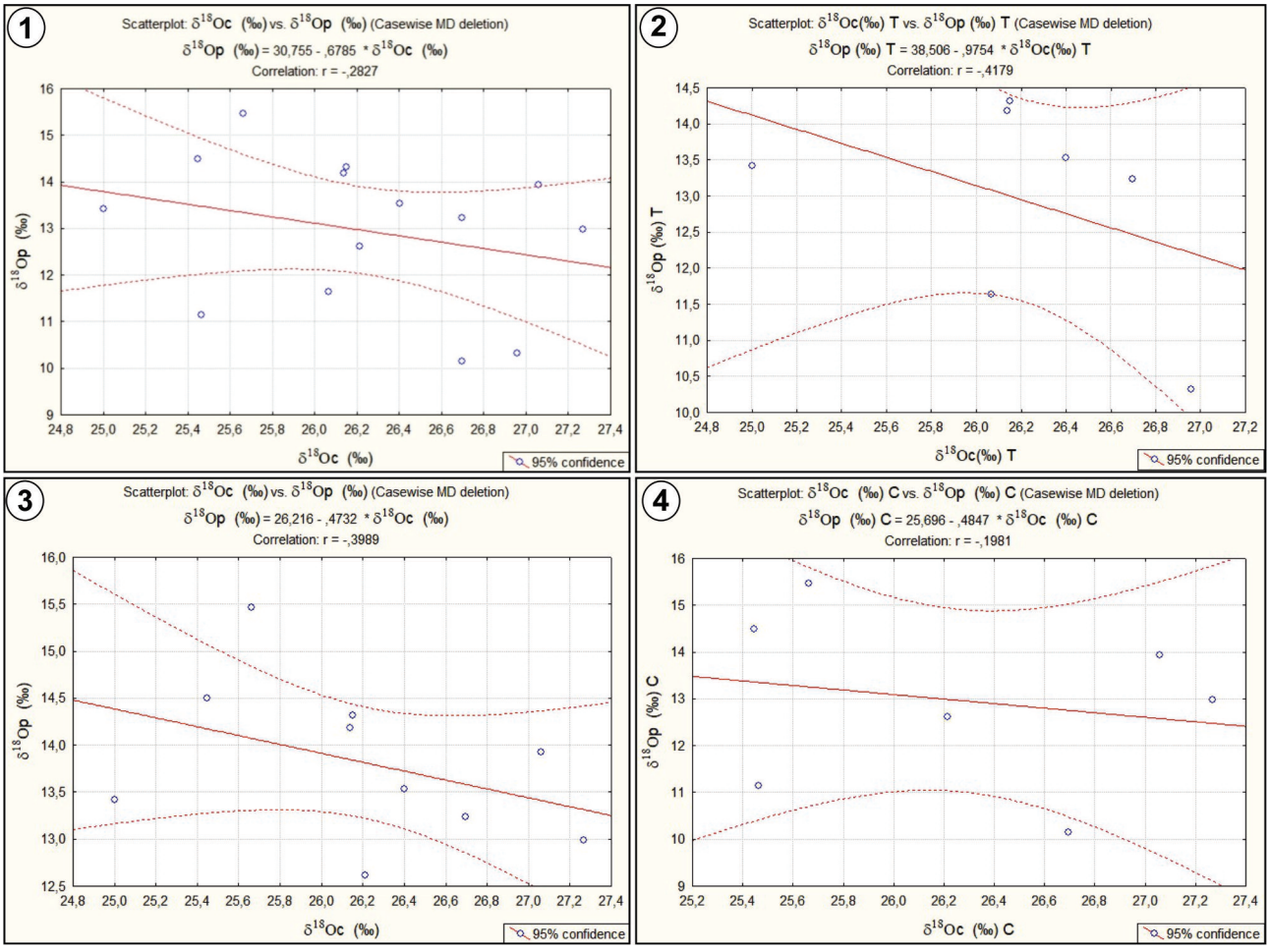

Figure 4. Linear regression graph of $\delta^{18}O_{CO3}$ (‰) and $\delta^{18}O_{PO4}$ (‰) values using different samples, all belonging to the La Cantera Formation (Aptian), San Luis Basin, San Luis Province, Argentina. **1,** All fish remains. **2,** Linear regression graph of $\delta^{18}O_{CO3}$ (‰) and $\delta^{18}O_{PO4}$ (‰) values of basal Actinopterygii. **3,** Linear regression graph of $\delta^{18}O_{CO3}$ (‰) and $\delta^{18}O_{PO4}$ (‰) values of Ganoid Neopterygii. **4,** Linear regression graph of $\delta^{18}O_{CO3}$ (‰) and $\delta^{18}O_{PO4}$ (‰) values according to the tissue sampled from fish remains.

However, our sample size is limited to further constrain paleoenvironmental variables such as atmospheric CO_2 (Arens & Jahren, 2000).

$\delta^{13}C_{CO2}$ composition

Calculations made applying Farquhar *et al.* (1989) equation for $\delta^{13}C_{CO2}$ present values that range between -2.6 and -6.1‰ with an average of -5.0‰. Calculations made following Arens & Jahren (2000) show $\delta^{13}C_{CO2}$ values that range between -9.18 and -5.81‰ with an average of -8.27‰ (Tab. 1).

Interpretation. According to previous reported values of $\delta^{13}C_{CO2}$ for the Cretaceous, the formula that best fits for the data of the La Cantera wood remains is the Farquhar *et al.* (1989) (-3.0‰ $\delta^{13}C$; Gröcke, 2002), meaning that the atmospheric carbon isotopic composition was on average approximately -5.0‰ $\delta^{13}C$.

Mineralogy

Bulk mineralogy. XRD analysis shows the presence of quartz, plagioclase, calcite, feldspar, analcime, and pyrite (Figs. 5, 6; Tab. 2). Calcite is the most abundant in the samples followed by quartz. The analcime is recorded throughout the section, as well as plagioclase and feldspar. Pyrite is only recorded in level 1 (Sample M3/18).

Clay mineral assemblages. Minerals identified in the mudstones of the La Cantera Formation are illite, kaolinite, chlorite, smectite, and mixed-layer illite/smectite. Each level analyzed presents a different combination of these minerals. Illite is recorded in each level tested, whereas chlorite is present in seven of eight levels tested, except for the level 2 (sample M4/18). Kaolinite is recorded in the lower section, until level 3 of the stratigraphical section sampled (Fig. 5). Mixed-layer illite/smectite is recorded throughout the section in six levels (Figs. 5, 7) while smectite is recorded only in levels 3 and 9 (Fig. 5).

Interpretation. All levels sampled contain illite. This clay mineral is the result of lixiviation and erosion, indicating high enhanced hydrolysis index due to high physical weathering (and low chemical weathering) compared to smectite or kaolinite (Chamley, 1989; Hillier *et al.*, 1995). The illite crystallinity is low, ruling out leaching and diagenesis processes (Fig. 7) (Fürsich *et al.*, 2005; Barrenechea *et al.*, 2018). The presence of smectite and mixed-layer illite/smectite indicates that precipitation was seasonal (Singer, 1984; Chamley, 1989).

There are no records of volcanic activity in the Late Aptian of the San Luis Basin, allowing to rule out volcanism as the origin for smectite (Do Campo *et al.*, 2010). However, we cannot discard the possibility of volcanic rocks in the source area as input for the smectite formation (Salduondo *et al.*, 2022). The mixed-layer illite/smectite is interpreted as an indicator of leaching (Moore & Reynolds, 1997). The lower level, which records assemblages with illite and kaolinite, indicate enhanced leaching due to a high-water regime

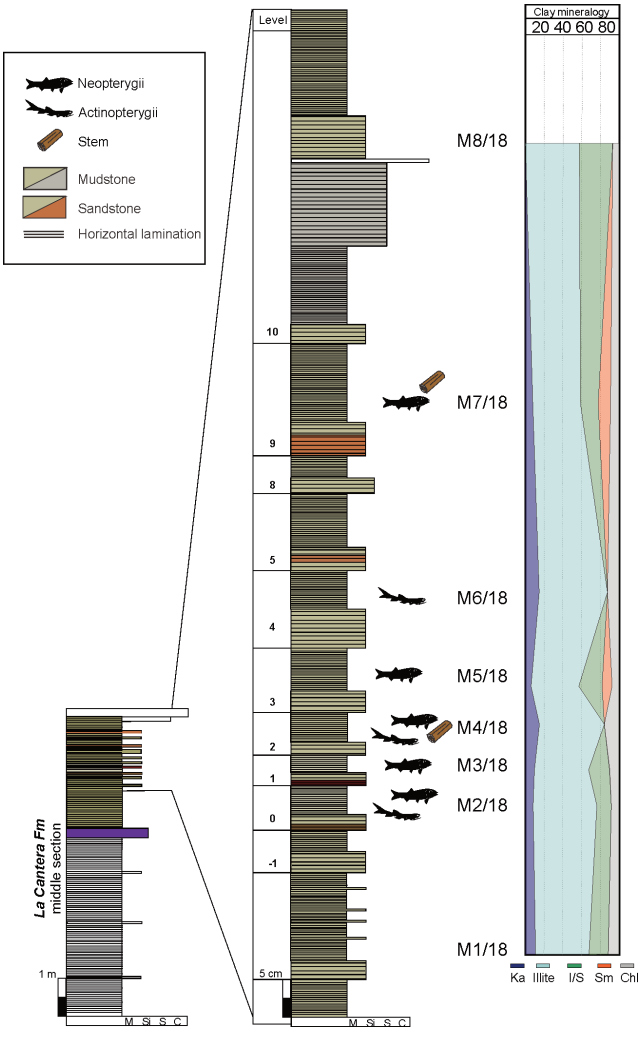

Figure 5. Sedimentary log of the middle section of the La Cantera Formation (Aptian) with clay mineralogy and fish and plant samples in its stratigraphic location. **I/S,** mixed-layer illite/smectite; **Sm,** smectite; **Kao,** Kaolinite; **Chl,** chlorite. **M**, mudstone; **Si**, siltstone; **S**, sandstone; **C**, conglomerate. M1/18: clay samples.

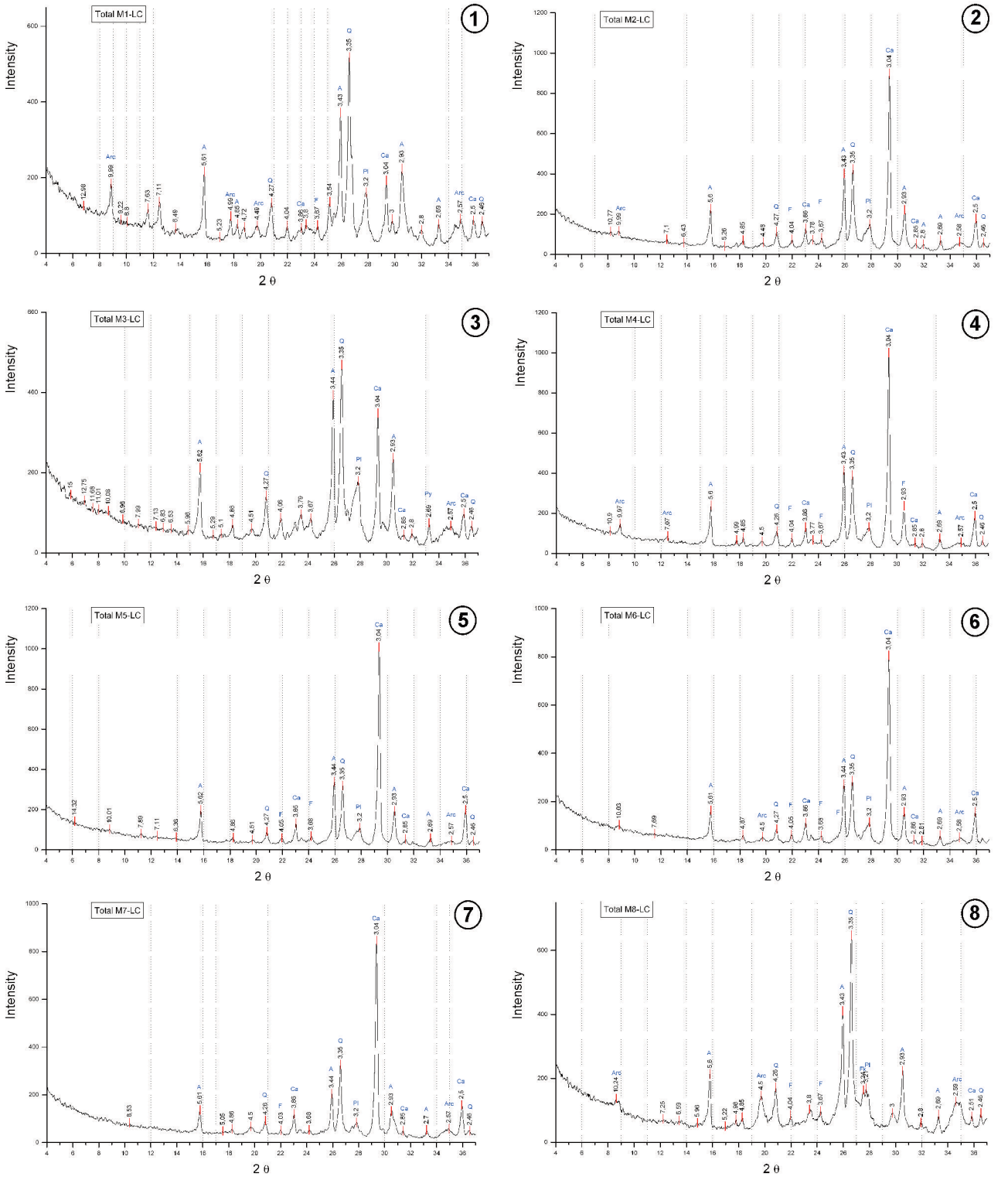

Figure 6. Total rock diffractograms of the La Cantera Formation (Aptian) mudstone samples in stratigraphical order showing: **Q,** quartz; **Pl,** plagioclase; **Ca,** calcite; **A,** analcime. **1,** Sample M1. **2,** Sample M2. **3,** Sample M3. **4,** Sample M4. **5,** Sample M5. **6,** Sample M6. **7,** Sample M7. **8,** Sample M8.

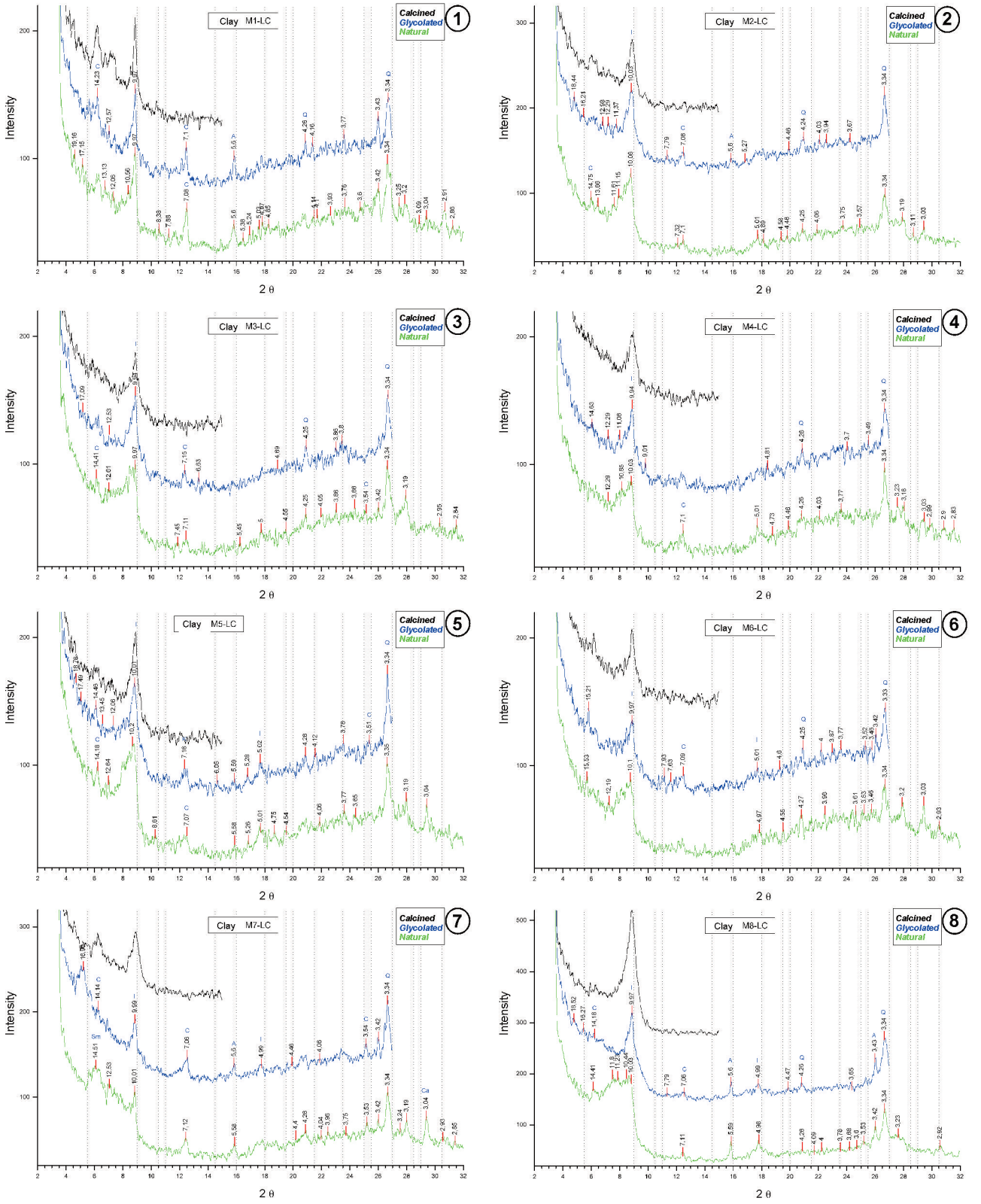

Figure 7. Oriented clay diffractograms of the La Cantera Formation (Aptian) mudstone samples in stratigraphical order under three different conditions: calcined, glycolated, and natural. Main peaks identified are: **I,** illite; **I/S,** illite/smectite; **K,** kaolinite; **S,** smectite; and **C,** chlorite. **1,** Sample M1. **2,** Sample M2. **3,** Sample M3. **4,** Sample M4. **5,** Sample M5. **6,** Sample M6. **7,** Sample M7. **8,** Sample M8.

under warm and humid conditions (Chamley, 1989). Chlorite characterizes all the samples as well; it is possible that along with illite, it is the result of smectite illitization and chloritization (Chamley, 1989). However, these processes characterize very high diagenetic stages, which is unlikely for our samples given the smectite presence in our samples. Therefore, the studied section was not submitted to significant deep burial and chlorite and illite are likely detrital in origin (Tineo *et al.*, 2022). It is interesting that calcite is an abundant mineral in the lacustrine deposits, because it indicates that lake waters were alkaline. It is possible that the abundant calcite content is linked to the gypsum found in more marginal facies that were subaerially exposed (Castillo Elías, 2016). An alkaline paleolake is also confirmed by the presence of analcime in the clay mineral assemblage, since it precipitates in alkaline waters in association with smectite; commonly, those conditions occur when there is a source of detrital volcanics (Chamley, 1989; Salduondo *et al.*, 2020). Moreover, recent mineralogical results from Triassic paleolakes have also reported analcime related to high input of volcaniclastic material and alkaline waters (Benavente *et al.*, 2015; Salduondo *et al.*, 2020).

DISCUSSION

Diagenetic overprint

In order to accurately interpret the different stable isotope datasets obtained from the fossil remains tested, it is necessary to conduct a diagenetic assessment. Therefore, the correlation-regression analysis of $\delta^{18}O_{CO3}$ and $\delta^{18}O_{PO4}$ was applied to fish remains. Since both components are formed from the same oxygen source, a positive correlation is expected between both $\delta^{18}O$ (Kolodny *et al.*, 1983; Iacumin *et al.*, 1996; Tütken *et al.*, 2006). In the case of the La Cantera fossil fish, the correlation coefficient found was r = -0.28, meaning that there is a negative correlation between $\delta^{18}O_{CO3}$ and $\delta^{18}O_{PO4}$ of 28%. This value is very low in comparison with other values for published datasets, like r = 0.76 obtained by Tütken *et al.* (2006) or r = 0.98 from Iacumin *et al.* (1996). Therefore, it is probable that the La Cantera fish remains analyzed present an altered isotopic signature to some extent. However, this does not assure that all values obtained have been diagenetically altered. As has been extensively discussed in the literature, PO_4 exchange is negligible in inorganic solutions (Kolodny *et al.*, 1983; Iacumin *et al.*, 1996).

The sampled tissues, such as dermal bones and elements associated with fins like fulcra, are covered by ganoine. Despite some authors proposing ganoine as a homologue tissue of tooth enamel of tetrapods (Qu *et al.*, 2015), the most accepted idea is that ganoine is an exclusive feature of Actinopterygii (Schultze, 1996, 2016), being different from true enamel considering its growth and histological arrangement (Schultze, 2018). Therefore, different formulas were applied to our data to rule out biases due to the nature of the sampled materials.

Paleotemperature calculations

Regarding the paleotemperature calculations obtained, the values resemble what has been found in the diagenesis assessment, since most of the values are reasonable for a water column in a shallow paleolake in a general warm paleoclimate context for the Early Cretaceous (Ufnar *et al.*, 2004). Five of the values obtained are unreasonably warm (40–45 °C) for most fishes to inhabit, implying that those remains suffered diagenetical reset. These samples represent the 30% of the data set and they don't imply the method used is not reliable, but probably there are external factors for the preservation of the isotopic signature that require further investigation.

Extant analogous ganoid Actinopterygii live up to 30 °C—*e.g.*, the gar *Lepisosteous oculatus* (Grande, 2010)—. Moreover, according to breeding places data, the bichires like *Polypterus senegalus* and *P. delhezi* tolerate a range of temperature between 24–28 °C. Besides, species of the basal actinopterygians Order Acipenseriformes can tolerate up to 20 °C, according to the Fish Base (Froese & Pauly, 2023). Alternatively, it is possible that during extremely low lake levels due to the dry season, temperatures became lethal for part of the biota. This has been documented in Lake Natron when lake levels descend to two or three m and water column temperatures rise to 35–45 °C. Considering other factors affecting the isotopic signature that might have led to paleotemperature anomalies (like physiology), the correlation-regression analysis was applied to each taxonomic group exclusively and to each tissue sampled, finding no difference in the results obtained. Nevertheless,

it is possible that the nature of the sampled material affected the preservation of the original isotopic composition and it has not been detected due to sample size. This might be a feasible possibility, since in Table 1 it is shown that the unreasonable paleotemperature values are from bones and some of the teeth, but particularly the ones that were attached to jaw fragments (bone).

That 70% of our dataset does reflect reasonable paleotemperature calculations (23.33–35.80 °C) is considered for the discussion as following. Within those values, there is no clear representation of a cold end member in the paleothermal range (minimum 23.33 °C). However, this would be expected in a warmer paleothermal context as has been described for the La Cantera Formation (Prámparo *et al.*, 2018). Even more, the La Cantera underfilled system most likely was of restricted extent, with low thermal mass and prone to heat easily in an arid context, similar to what has been observed for modern lakes (Woolway & Merchant, 2017). The paleotemperature values found are very similar to temperatures measured during the last decades for modern lakes in Africa and Asia in extensional tectonic context, like Lake Kivu (surface: 2,370 km^2, T = 23 °C); Lake Turkana (surface: 7,785 km^2, T = 28.5 °C); Lake Chilka (surface: 885 km^2, T = 25 °C); and Lake Upemba (surface: 573 km^2, T = 26 °C) (Liu *et al.*, 2019). Paleotemperatures interpreted as reasonable for the La Cantera water column are also in agreement with values found for other Cretaceous lacustrine deposits from USA, in which temperatures reaching 37.8 °C have been obtained from lacustrine carbonates (Fetrow *et al.*, 2022).

This implies that the stable isotope signature of fish remains could be used to some extent as a paleoclimate proxy coupled with other reliable paleoclimate proxies and applying diagenesis assessment to the data retrieved. Consistently with that, $\delta^{13}C$ values obtained from plant remains from the La Cantera Formation (average: -25‰) are remarkably similar to the average $\delta^{13}C$ of modern C3 plants (-25.4‰) (Craig, 1954), wood in particular (Gröcke, 2002) which is consistent with the sampled stems. These strongly suggests that plant remains preserve the isotopic primary signature. However, the number of specimens that pass the preservation analysis was low, so preservation is a significant and limiting factor to consider to further test this proxy. Our dataset has an average approximate $\delta^{13}C_{CO2}$ composition of -5.0‰ $\delta^{13}C$. This matches previous values obtained for the Cretaceous of -3.0‰ $\delta^{13}C$ (Gröcke, 2002), supporting that with careful and extensive sampling, the La Cantera plant fossils would allow exploring regional climate variables such as $\delta^{13}C$ of atmospheric CO_2 (Arens & Jahren, 2000; Gröcke, 2002). Furthermore, according to modern experiments on C3 plants, the values we have found would correspond to CO_2 enrichment conditions (Beerling & Woodward, 1995).

Mineralogical proxies

Regarding the clay mineral assemblage of the La Cantera mudstones, most of the analyzed samples are enriched in mixed-layer illite/smectite (I/S). This could be related with the progressive transformation of smectite to illite during burial (Hower *et al.*, 1976). Therefore, it is possible that I/S is related with the presence of former smectite and consequently reflecting relatively warm-subarid conditions (alternation of wet and dry seasons) in the hinterlands (Chamley, 1989). Overall, most of the samples from the studied section are dominated by illite and chlorite, and to a lesser extent by kaolinite and I/S. Illite and chlorite are usually associated with relatively low chemical weathering forming through physical weathering (*e.g.*, Chamley, 1989; Hillier *et al.*, 1995; Tineo *et al.*, 2022).

These results point to an increased hydrolysis index, meaning significant seasonal rainfall (Singer, 1984; Chamley, 1989). Similar interpretations have been obtained from clay assemblages of the Cretaceous of Salta Province, north of Argentina (Do Campo *et al.*, 2010). A seasonal context is in agreement with a shallow lake that probably lowered its water column during the dry season, fluctuating from warm to warmer temperatures, like it is indicated by the paleotemperature dataset obtained. The clay mineral assemblage interpretation is also in agreement with previous paleoclimate interpretations made from palynological studies that found *Classopolis* and Gnetales specimens, indicating aridity episodes during La Cantera deposition (Prámparo *et al.*, 2018). Even more, there are several studies recording warm paleotemperatures and aridity conditions for mid–Cretaceous globally (Fetrow *et al.*, 2022) and particularly for terrestrial ecosystems during the Aptian–Albian (Ludvigson *et al.*, 2015).

Another significant sedimentological feature of the La Cantera deposits is that it contains abundant primary gypsum deposits in other sections of the unit throughout the finely laminated mudstones. These have led to the interpretation of an underfilled lake basin type for the La Cantera lacustrine system (Castillo Elías, 2016) *sensu* Bohacs *et al.* (2000), in which evaporites characterize the sedimentary column. This provides a coherent general context for the information we have found in this study.

CONCLUSIONS

The paleontological dataset from the La Cantera Formation (fish and macroflora) is a useful and accurate mean of developing paleoclimate proxies. Fish remains preserve the primary isotopic signature partially. Therefore, coupled with other paleoclimate proxies and with rigorous diagenesis tests, it can potentially be applied for paleoclimate reconstructions for this system. Plant remains remarkably preserve the original isotopic signature in the range of modern C3 plants and allow constraining paleoclimate and paleoenvironmental conditions. Furthermore, they constitute a potential proxy for deep time local C biogeochemical cycle reconstruction and global $\delta^{13}C_{CO2}$ composition, since our results show agreement with other localities atmospheric CO_2 carbon isotopic composition during the Cretaceous. Therefore, these remains should be further investigated.

The isotopic signature from unaltered fish remains allowed obtaining a paleothermal range of 23.33–35.8 °C for the water column of the La Cantera paleolake. These values are warm with a high minimum temperature, in agreement with the Lower Cretaceous global paleoclimate context in which maximum heat gain due to latent heat flux during a hothouse occurred at ~50 °N, at an equivalent paleolatitudinal range of the La Cantera lacustrine system in the Southern Hemisphere. Our data also agrees locally with an underfilled lake basin development in an intracontinental rift basin. Clay mineral assemblage composition indicates a seasonal rainfall distribution that supports the development of an underfilled paleolake that experienced seasonal low lake levels, warming up its water column. This is in agreement with previous palynological and sedimentological interpretations of aridity for the La Cantera Formation.

ACKNOWLEDGEMENTS

We thank Dr. Gómez (UNSL) for assistance with fossil plant sampling and Drs. Comerio and Pérez for their thorough revision that improved the manuscript. Funding: PROICO 340103 Universidad Nacional de San Luis (ABA). We are grateful for Drs. Cariglino, Viglino and Carabajal editorial work.

REFERENCES

Abell, P. I., Awramik, S. M., Osborne, R. H., & Tomellini, S. (1982). Plio–Pleistocene lacustrine stromatolites from lake Turkana, Kenya: Morphology, stratigraphy and stable isotopes. *Sedimentary Geology*, *32*(1–2), 1–26. https://doi.org/10.1016/0037-0738(82)90011-2

Amiot, R., Wang, X., Lécuyer, C., Buffetaut, E., Boudad, L., Cavin, L., & Zhang, F. (2010). Oxygen and carbon isotope compositions of middle Cretaceous vertebrates from North Africa and Brazil: Ecological and environmental significance. *Palaeogeography, Palaeoclimatology, Palaeoecology*, *297*(2), 439–451. https://doi.org/10.1016/j.palaeo.2010.08.027

Arcucci, A. B., Prámparo, M. B., Codorniú, L., Giordano, P. G., Castillo Elías, G., Puebla, G., Mego, N., Gómez, M., & Bustos Escalona, E. (2015). Biotic assemblages from Lower Cretaceous lacustrine systems, San Luis Basin, central-western Argentina. *Boletín Geológico y Minero de España*, *126*(1), 109–128.

Arens, N. C. & Jahren, A. H. (2000). Carbon isotope excursion in atmospheric CO^2 at the Cretaceous–Tertiary boundary: Evidence from terrestrial sediments. *Palaios*, *15*, 314–322. https://doi.org/10.1669/0883-1351(2000)015<0314:CIEIAC>2.0.CO;2

Barrenechea, J. E., López-Gómez, J., & De La Horra, R. (2018). Sedimentology, clay mineralogy and palaeosols of the mid–Carnian Pluvial Episode in eastern Spain: insights into humidity and sea level variations. *Journal of the Geological Society*, *175*, 993–1003. https://doi.org/10.1144/jgs2018-024

Beerling, D. J. & Woodward, F. I. (1995). Leaf stable carbon isotope composition records increased water-use efficiency of C3 plants in response to atmospheric CO_2 enrichment. *Functional Ecology*, *9*(3), 394–401. https://doi.org/10.2307/2390002

Benavente, C. A., Mancuso, A. C., & Bohacs, K. M. (2019). Paleohydrogeologic reconstruction of Triassic carbonate paleolakes from stable isotopes: Encompassing two lacustrine models. *Journal of South American Earth Sciences*, *95*, 102292. https://doi.org/10.1016/j.jsames.2019.102292

Benavente, C. A., Mancuso, A. C., & Bohacs, K. M. (2021). Chapter 14, Reconstructing paleoenvironmental conditions through integration of paleogeography, stratigraphy, sedimentology, mineralogy, and stable isotope data of lacustrine carbonates—an example from early Middle Triassic strata of southwest Gondwana, Cuyana Rift, Argentina. In M. R. Rosen, L. Park-Bousch, D. B. Finkelstein, & S. Pla-Pueyo (Eds.), *Limnogeology: Progress, challenges and opportunities: A tribute to Beth Gierlowski-Kordesch* (pp. 471–509). Springer International Publishing. http://doi.org/10.1007/978-3-030-66576-0_16

Benavente, C. A., Mancuso, A. C., Cabaleri, N. G., & Gierlowski-Kordesch, E. H. (2015). Comparison of lacustrine successions and their paleohydrologic implications in the two sub-basins of the Triassic Cuyana rift, Argentina, *Sedimentology*, *62*, 1771–1813. https://doi.org/10.1111/sed.12209

Benavente, C. A., Mancuso, A. C., Irmis, R. B., Bohacs, K. M., & Matheos, S. (2022). Tectonically conditioned record of continental interior paleoclimate during the Carnian Pluvial Event: the Upper Triassic Los Rastros Formation, Argentina. *Geological Society of America Bulletin*, *134*(1–2), 60–80. https://doi.org/10.1130/B35847.1

Bergner, A. G. N., Strecker, M. R., Trauth, M. H., Deino, A., Gasse, F., Blisniuk, P., & Dühnforth, M. (2009). Tectonic and climatic control on evolution of rift lakes in the central Kenya Rift, East Africa. *Quaternary Science Reviews*, *28*, 2804–2816. https://doi.org/10.1016/j.quascirev.2009.07.008

Bessems, I., Verschuren, D., Russell, J. M., Hus, J., Mees, F., & Cumming, B. F. (2008). Palaeolimnological evidence for widespread late 18th century drought across equatorial East Africa. *Palaeogeography, Palaeoclimatology, Palaeoecology*, *259*, 107–120. https://doi.org/10.1016/j.palaeo.2007.10.002

Bohacs, K. M., Carroll, A. R., Neal, J. E., & Mankiewicz, P. J. (2000). Lake-basin type, source potential, and hydrocarbon character: an integrated sequence-stratigraphic-geochemical framework. Lake basins through space and time. *American Association of Petroleum Geologists Studies in Geology*, *46*, 3–34. https://doi.org/10.1306/St46706C1

Bowen, G. J. & Wilkinson, B. (2002). Spatial distribution of $\delta^{18}O$ in meteoric precipitation. *Geology*, *30*, 315–318. https://doi.org/10.1130/0091-7613(2002)030<0315:SDOOIM>2.0.CO;2

Castillo Elías, G. (2016). *Aspectos paleoecológicos y sedimentológicos de la Formación La Cantera, Sierra del Gigante, Aptiano Tardío, Sierras de San Luis.* [PhD Thesis, Facultad de Ciencias Exactas y Naturales, Universidad Nacional de San Luis].

Cerling, T. E., Bowen G. J., Ehleringer J. R., & Sponheimer, M. (2007). The reaction progress variable and isotope turnover in biological systems. *Terrestrial Ecology*, *1*, 163–171. https://doi.org/10.1016/S1936-7961(07)01011-1

Chamley, H. (1989). *Clay Sedimentology*. Springer.

Craig, H. (1954). Carbon 13 in plants and the relationships between carbon 13 and carbon 14 variations in nature. *The Journal of Geology*, *62*(2), 115–149. https://doi.org/10.1086/626141

Criado-Roque, P., Mombrú, C., & Moreno, J. (1981). Sedimentitas mesozoicas. Geología de la Provincia de San Luis. In *Relatorio del VIII Congreso Geológico Argentino* (pp. 79–96). Asociación Geológica Argentina.

Do Campo, M., del Papa, C., Nieto, F., Hongn, F., & Petrinovic, I. (2010). Integrated analysis for constraining palaeoclimatic and volcanic influences on clay–mineral assemblages in orogenic basins (Palaeogene Andean foreland, Northwestern Argentina). *Sedimentary Geology*, *228*(3–4), 98–112. https://doi.org/10.1016/j.sedgeo.2010.04.002

Farquhar, G. D., Hubick, K. T., Condon, A. G., & Richards, R. A. (1989). Carbon isotope fractionation and plant water-use efficiency. In W. Rundel, J. R. Ehleringer, & K. A. Nagy (Eds.), *Stable isotopes in ecological research* (pp. 21–40). Springer.

Fetrow, A. C., Snell, K. E., Di Fiori, R. V., Long, S. P., & Bonde, J. W. (2022). How hot is too hot? Disentangling mid–Cretaceous hothouse paleoclimate from diagenesis. *Paleoceanography and Paleoclimatology*, *37*, e2022PA004517. https://doi.org/10.1029/2022PA004517

Flores, M. A. (1969). El Bolsón de las Salinas en la provincia de San Luis. *Abstracts of the 4° Jornadas Geológicas Argentinas* (vol. 1, pp. 311–327). Mendoza.

Froese, R. & Pauly, D. Editors. (2023). *FishBase,* version 02/2023. Retrieved December 2022, fromhttps://www.fishbase.se/search.php

Fürsich, F. T., Singh, I. B., Joachimski, M., Krumm, S., Schlirf, M., & Schlirf, S. (2005). Palaeoclimate reconstructions of the Middle Jurassic of Kachchh (western India): an integrated approach based on palaeoecological, oxygen isotopic, and clay mineralogical data. *Palaeogeography, Palaeoclimatology, Palaeoecology*, *217*, 289–309. https://doi.org/10.1016/j.palaeo.2004.11.026

Gierlowski-Kordesch, E. & Kelts, K. (1994). *Global geological record of lake basins*. Cambridge University Press.

Giordano, P. G., Arratia, G., & Schultze, H. P. (2016). Scale morphology and specialized dorsal scales of a new teleosteomorph fish from the Aptian of West Gondwana. *Fossil Record*, *19*, 61–81. https://doi.org/10.5194/fr-19-61-2016

Grande, L. (2010). An empirical synthetic pattern study of gars (Lepisosteiformes) and closely related species, based mostly on skeletal anatomy. The resurrection of Holostei. *Copeia*, *10*(2A), 1–871.

Grimes, S. T., Mattey, D. P., Hooker, J. J., & Collinson, M. E. (2003). Paleogene paleoclimate reconstruction using oxygen isotopes from land and freshwater organisms: the use of multiple paleoproxies. *Geochimica et Cosmochimica*, *67*(21), 4033–4047. https://doi.org/10.1016/S0016-7037(03)00173-X

Gröcke, D. R. (2002). The carbon isotope composition of ancient CO_2 based on higher-plant organic matter. *Philosophical Transactions of the Royal Society of London A*, *360*, 633–658. https://doi.org/10.1098/rsta.2001.0965

Hillier, S., Matyas, J., Matter, A., & Vasseur, G. (1995). Illite/smectite diagenesis and its variable correlation with vitrinite reflectance in the Pannonian Basin. *Clays and Clay Minerals*, *43*(2), 174–183.

Hower, J., Eslinger, E. V., Hower, M. E., & Perry, E. A. (1976). Mechanism of burial metamorphism of argillaceous sediment. 1. Mineralogical and chemical evidence. *Geological Society of America Bulletin*, *87*, 725–737. https://doi.org/10.1130/0016-7606(1976)87<725:MOBMOA>2.0.CO;2

Iacumin, P., Bocherens, H., Mariotti, A., & Longinelli, A. (1996). Oxygen isotope analyses of co-existing carbonate and phosphate in biogenic apatite: a way to monitor diagenetic alteration of bone phosphate. *Earth and Planetary Science Letters*, *142*(1–2), 1–6. https://doi.org/10.1016/0012-821X(96)00093-3

Kolodny, Y., Luz, B., & Navon, O. (1983). Oxygen isotope variations in phosphate of biogenic apatites, I. Fish bone apatite—rechecking the rules of the game. *Earth and Planetary Science Letters*, *64*(3), 398–404. https://doi.org/10.1016/0012-821X(83)90100-0

Leng, M. J., Lamb, A. L., Heaton, T. H. E., Marshall, J. D., Wolfe, B. B., Jones, M. D., Holmes, J., & Arrowsmith, A. (2005). Isotopes in lake sediments. *Isotopes in Palaeoenvironmental Research*, *10*, 147–184.

Liu, B., Wan, W., Xie, H., Li, H., Zhu, S., Zhang, G., & Hong, Y. (2019). A long-term dataset of lake surface water temperature over the Tibetan Plateau derived from AVHRR 1981–2015. *Scientific data*, *6*(1), 48. https://doi.org/10.1038/s41597-019-0040-7

Longinelli, A. & Nuti, S. (1973). Oxygen isotope measurements of phosphate from fish teeth and bones. *Earth and Planetay Science Letters*, *20*(3), 337–340. https://doi.org/10.1016/0012-821X(73)90007-1

Ludvigson, G. A., Joeckel, R. M., Murphy, L. R., Stockli, D. F., Gonzalez, L. A., Suarez, C. A., Kirkland, J. I., & Al-Suwaidi, A. (2015). The emerging terrestrial record of Aptian–Albian global change. *Cretaceous Research*, *56*, 1–24. https://doi.org/10.1016/j.cretres.2014.11.008

Michener, R. & Lajtha, K. (2008). *Stable isotopes in ecology and environmental science.* Blackwell Publishing.

Moernaut, J., Verschuren, D., Charlet, F., Kristen, I., Fagot, M., & De Batist, M. (2010). The seismic-stratigraphic record of lake-level fluctuations in Lake Challa: hydrological stability and change in equatorial East Africa over the last 140 kyr. *Earth and Planetary Science Letters*, *290*, 214–223. https://doi.org/10.1016/j.epsl.2009.12.023

Moore, D. M. & Reynolds Jr., R. C. (1997). *X-Ray Diffraction and the Identification and Analysis of Clay Minerals*. Oxford University Press.

Pereira, N. S., Sial, A. N., Pinheiro, P. B., Freitas, F. L., & Silva, A. (2021). Carbon and oxygen stable isotopes of freshwater fish otoliths from the São Francisco River, northeastern Brazil. *Anais da Academia Brasileira de Ciências*, *93*, e20191050. https://doi.org/10.1590/0001-3765202120191050

Petrulevičius, J., Nel, A., & Sallenave, S. (2010). Recent genus *Notonecta* (Insecta: Heteroptera: Notonectidae) in the Lower Cretaceous of San Luis, Argentina: Palaeoecological implications. *International Journal of Entomology*, *46*, 1–2. https://doi.org/10.1080/00379271.2010.10697665

Prámparo, M. B. (1994). Lower Cretaceous palynoflora of the La Cantera Formation, San Luis Basin: correlation with other Cretaceous palynofloras of Argentina. *Cretaceous Research*, *15*(2), 193–203. https://doi.org/10.1006/cres.1994.1010

Prámparo, M. B. (2012). Non-marine Cretaceous palynomorph biostratigraphy of Argentina: a brief summary. *Journal of Stratigraphy*, *36*, 213–228.

Prámparo, M. B., Vento, B., Narváez, P. L., Mego, N., & Puebla, G. G. (2018). Cretaceous climatic reconstruction from Argentina based on palynological data. *Boletín Geológico Minero*, *129*, 615–631. http://dx.doi.org/10.21701/bolgeomin.129.4.002

Pucéat, E., Joachimski, M. M., Bouilloux, A., Monna, F., Bonin, A., Motreuil, S., & Quesne, D. (2010). Revised phosphate–water fractionation equation reassessing paleotemperatures derived from biogenic apatite. *Earth and Planetary Science Letters*, *298*(1–2), 135–142. https://doi.org/10.1016/j.epsl.2010.07.034

Puebla, G. (2009). A new angiosperm leaf morphotype from the Early Cretaceous (Late Aptian) of San Luis Basin, Argentina. *Ameghiniana*, *46*, 557–566.

Puebla, G., Mego, N., & Prámparo, M. (2012). Asociación de Briófitas de la Formación La Cantera, Aptiano Tardío, Cuenca de San Luis, Argentina. *Ameghiniana*, *49*(2), 217–229. https://doi.org/10.5710/AMGH.v49i2(504)

Qu, Q., Haitina, T., Zhu, M., & Ahlberg, P. E. (2015). New genomic and fossil data illuminate the origin of enamel. *Nature*, *526*(7571), 108–111.

Rey, K., Day, M. O., Amiot, R., Fourel, F., Luyt, J., Lécuyer, C., & Rubidge, B. S. (2020). Stable isotopes ($\delta^{18}O$ and $\delta^{13}C$) give new perspective on the ecology and diet of *Endothiodon bathystoma* (Therapsida, Dicynodontia) from the late Permian of the South African Karoo Basin. *Palaeogeography, Palaeoclimatology, Palaeoecology*, *556*, 109882. https://doi.org/10.1016/j.palaeo.2020.109882

Rivarola, D. & Spalletti, L. (2006). Modelo de sedimentación continental para el rift Cretácico de la Argentina central. Ejemplo de la Sierra de Las Quijadas, San Luis. *Revista de la Asociación Geológica Argentina*, *61*(1), 63–80.

Salduondo, J., Comerio, M., Pineda, J. A., Cravero, F., & Erra, G. (2022). Palaeoclimatic and diagenetic controls based on clay mineralogy and organic matter distribution: The continental rift Cuyo Basin (Triassic), west-central Argentina. *Sedimentology*, *69*, 2867–2896. https://doi.org/10.1111/sed.13023

Schultze, H. P. (1996). Morphologische und histologische Untersuchungen an Schuppen mesozoischer Actinopterygier (Übergang von Ganoid zu-Rundschuppen). *Neuss Jahrbuch für Geologie und Palaontologie*, *126*(3), 232–314.

Schultze, H. P. (2016). Scales, enamel, cosmine, ganoine, and early osteichthyans. *Comptes Rendus Palevol*, *15*(1–2), 83–102. https://doi.org/10.1016/j.crpv.2015.04.001

Schultze, H. P. (2018). Hard tissues in fish evolution: history and current issues. *Cybium*, *42*(1), 29–39.

Singer, A. (1984). The paleoclimatic interpretation of clay minerals in sediments—a review. *Earth-Science Reviews*, *21*(4), 251–293. https://doi.org/10.1016/0012-8252(84)90055-2

Sisma-Ventura, G., Tütken, T., Peters, S. T., Bialik, O. M., Zohar, I., & Pack, A. (2019). Past aquatic environments in the Levant inferred from stable isotope compositions of carbonate and phosphate in fish teeth. *Plos ONE*, *14*(7), e0220390. https://doi.org/10.1371/journal.pone.0220390

Tieszen, L., Boutton, T. W., & Tesdahl, K. G. (1983). Fractionation and turnover of stable carbon isotopes in animal tissues: Implications for $\delta^{13}C$ analysis of diet. *Oecologia*, *57*, 32–37. https://doi.org/10.1007/BF00379558

Tineo, D. E., Comerio, M. A., Vigiani, L. H., Kürten Moreno, G. S., & Poiré, D. G. (2022). Tectonic and paleoclimatic controls on the composition of inland wetland deposits, Chaco foreland basin, Central Andes. *Journal of Sedimentary Research*, *92*(2), 112–133. https://doi.org/10.2110/jsr.2021.033

Tütken, T., Vennemann, W., Janz, H., & Heizmann, E. P. J. (2006). Palaeoenvironment and palaeoclimate of the Middle Miocene lake in the Steinheim basin, SW Germany: A reconstruction from C, O, and Sr isotopes of fossil remains. *Palaeogeography, Palaeoclimatology, Palaeoecology*, *241*, 457–491. https://doi.org/10.1016/j.palaeo.2006.04.007

Ufnar, D. F., González, L. A., Ludvigson, G. A., Brenner, R. L., & Witzke, B. J. (2004). Evidence for increased latent heat transport during the Cretaceous (Albian) greenhouse warming. *Geology*, *32*(12), 1049–1052. https://doi.org/10.1130/G20828.1

van Hinsbergen, D. J., de Groot, L. V., van Schaik, S. J., Spakman, W., Bijl, P. K., Sluijs, A., & Brinkhuis, H. (2015). A paleolatitude calculator for paleoclimate studies. *Plos ONE*, *10*(6), e0126946. https://doi.org/10.1371/journal.pone.0126946

Wang, L., Scarpitta, S. C., Zhang, S. C., & Zheng, M. P. (2002). Later Pleistocene/Holocene climate conditions of Qinghai–Xizhang Plateau (Tibet) based on carbon and oxygen stable isotopes of Zabuye Lake sediments. *Earth and Planetary Science Letters*, *203*(1), 461–477. https://doi.org/10.1016/S0012-821X(02)00829-4

West, J. B., Bowen, G. J., Cerling, T. E., & Ehleringer, J. R. (2006). Stable isotopes as one of nature's ecological recorders. *Trends in Ecology*, *21*(7), 408–414. https://doi.org/10.1016/j.tree.2006.04.002

Woolway, R. I. & Merchant, C. J. (2017). Amplified surface temperature response of cold, deep lakes to inter-annual air temperature variability. *Scientific Reports*, *4*(7), 1–8. https://doi.org/10.1038/s41598-017-04058-0

Yrigoyen, M. R. (1975). La edad cretácica del Grupo Gigante (San Luis) y su relación con cuencas circunvecinas. *Abstracts of I Congreso Argentino de Paleontología y Bioestratigrafía, vol. 2* (pp. 29–56). San Miguel de Tucumán.

doi: 10.5710/PEAPA.17.04.2023.454

Recibido: 25 de enero 2023
Aceptado: 17 de abril 2023
Publicado: 09 de agosto 2023